Extension and contraction within volcanically buried impact craters and basins on Mercury

Thomas R. Watters[1]*, Sean C. Solomon[2], Christian Klimczak[2], Andrew M. Freed[3], James W. Head[4], Carolyn M. Ernst[5], David M. Blair[3], Timothy A. Goudge[4], and Paul K. Byrne[2]

[1]Center for Earth and Planetary Studies, National Air and Space Museum, Smithsonian Institution, Washington, DC 20560, USA
[2]Department of Terrestrial Magnetism, Carnegie Institution of Washington, Washington, DC 20015, USA
[3]Department of Earth and Atmospheric Sciences, Purdue University, West Lafayette, Indiana 47907, USA
[4]Department of Geological Sciences, Brown University, Providence, Rhode Island 02912, USA
[5]The Johns Hopkins University Applied Physics Laboratory, Laurel, Maryland 20723, USA

ABSTRACT

Orbital images of Mercury obtained by the MESSENGER spacecraft have revealed families of troughs, interpreted to be graben, on volcanic plains material that largely or completely buried preexisting craters and basins. The graben are partially to fully encircled by rings of contractional wrinkle ridges localized over the rims of the buried impact features to form systems of associated contractional and extensional landforms. Most of the buried craters and basins with graben identified to date are located in the extensive volcanic plains that cover much of Mercury's northern high latitudes. The distinctive relationship between wrinkle ridges and graben in buried craters and basins on Mercury is interpreted to be the result of a combination of extensional stresses from cooling and thermal contraction of thick lava flow units and compressional stresses from cooling and contraction of the planet's interior.

INTRODUCTION

Images obtained during flybys of Mercury by the Mariner 10 and the MErcury Surface, Space ENvironment, GEochemistry, and Ranging (MESSENGER) spacecraft revealed widespread evidence of contractional deformation (e.g., Strom et al., 1975; Solomon et al., 2008; Watters et al., 2009a). Documented evidence for extensional deformation on Mercury was principally confined to smooth plains in the interiors of several major impact basins (e.g., Strom et al., 1975; Melosh and McKinnon, 1988; Solomon et al., 2008; Murchie et al., 2008; Watters et al., 2009b, 2009c; Prockter et al., 2010). Insertion of MESSENGER into orbit around Mercury in March 2011 has permitted high-resolution imaging of the planet's surface on a global basis. Here, we describe families of troughs, interpreted to be graben, seen for the first time in these orbital images. Unlike the previously seen extensional features, these graben formed on volcanic plains material that largely or completely buried preexisting craters and basins.

Many of the examples of this newly seen setting for extensional deformation are in Mercury's northern smooth plains (Fig. 1), an area not fully imaged during the flybys. Like other large smooth plains units on Mercury, such as those exterior to the Caloris basin (Robinson et al., 2008; Head et al., 2008; Denevi et al., 2009; Watters et al., 2009a, 2009b), the northern plains consist of flood volcanic deposits deformed by contractional wrinkle ridges (Head et al., 2011). We describe these extensional landforms, seen locally on the plains exterior to Caloris as well as the northern plains, and their relation to wrinkle ridges. With finite element models we then test several possible hypotheses for the formation of these coupled extensional-contractional tectonic systems.

CHARACTERISTICS OF EXTENSIONAL-CONTRACTIONAL TECTONIC SYSTEMS

Narrow linear and curvilinear troughs that occur locally on Mercury's northern plains and plains exterior to Caloris (Figs. 2 and 3) are interpreted to be graben on the basis of morphology (i.e., relatively steep walls and flat floors that shoal toward the trough ends) and evidence of fault segment linkage indicated by en echelon step-over geometries. The graben typically occur in areas of plains that are partly to completely encircled by a ring of wrinkle ridges. Such rings are common in volcanic plains on Mercury and other terrestrial planets, and are attributed to strain localization above the rim crests of "ghost" impact structures that have been fully buried by lava flows (Head et al., 2008; Watters et al., 2009a). We describe examples that illustrate the relationships between extensional and contractional landforms in these tectonic systems. (Further information is available in the GSA Data Repository[1].)

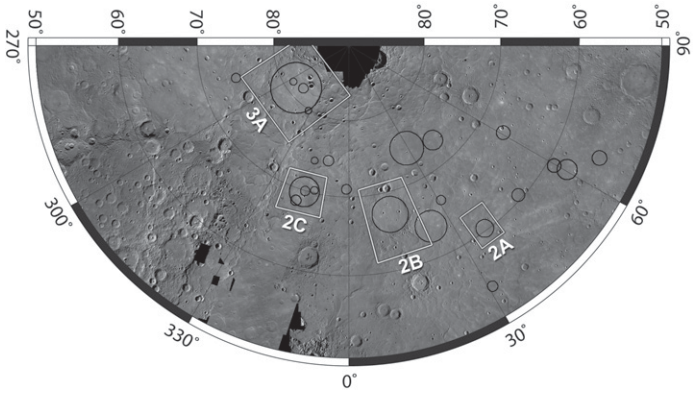

Figure 1. Mosaic of Mercury Dual Imaging System (MDIS) images of part of the high northern latitudes of Mercury. The region is dominated by volcanic smooth plains. Locations of buried impact craters and basins that contain graben enclosed by a wrinkle-ridge ring are indicated by black circles. Locations of Figures 2A, 2B, 2C, and 3A are also shown.

Northern Plains

In one example of these tectonic assemblages, shown in Figure 2A, graben form polygonal patterns with polygon widths of up to ~10 km, similar to the dimensions of polygons formed by graben in the Caloris and Rembrandt basins (Watters et al., 2009b, 2009c). The largest graben in this assemblage is up to ~1 km wide and ~15 km long. Wrinkle ridges on the plains outside of the buried crater terminate at its ridge ring but do not cross into the interior plains (Fig. 2A). No prominent wrinkle ridges are seen in the plains within the ghost crater.

Another buried impact structure inferred on the basis of exposed rim massifs and a series of curvilinear wrinkle ridges hosts a complex array of graben concentrated in its central area (Fig. 2B). Here, graben also form polygonal patterns, but the number of polygons is greater and their widths are smaller (<10 km). The scale of the largest graben is similar to that in the

*E-mail: watterst@si.edu.

[1]GSA Data Repository item 2012323, description of the spatial distribution of the tectonic systems, and supporting figures, is available online at www.geosociety.org/pubs/ft2012.htm, or on request from editing@geosociety.org or Documents Secretary, GSA, P.O. Box 9140, Boulder, CO 80301, USA.

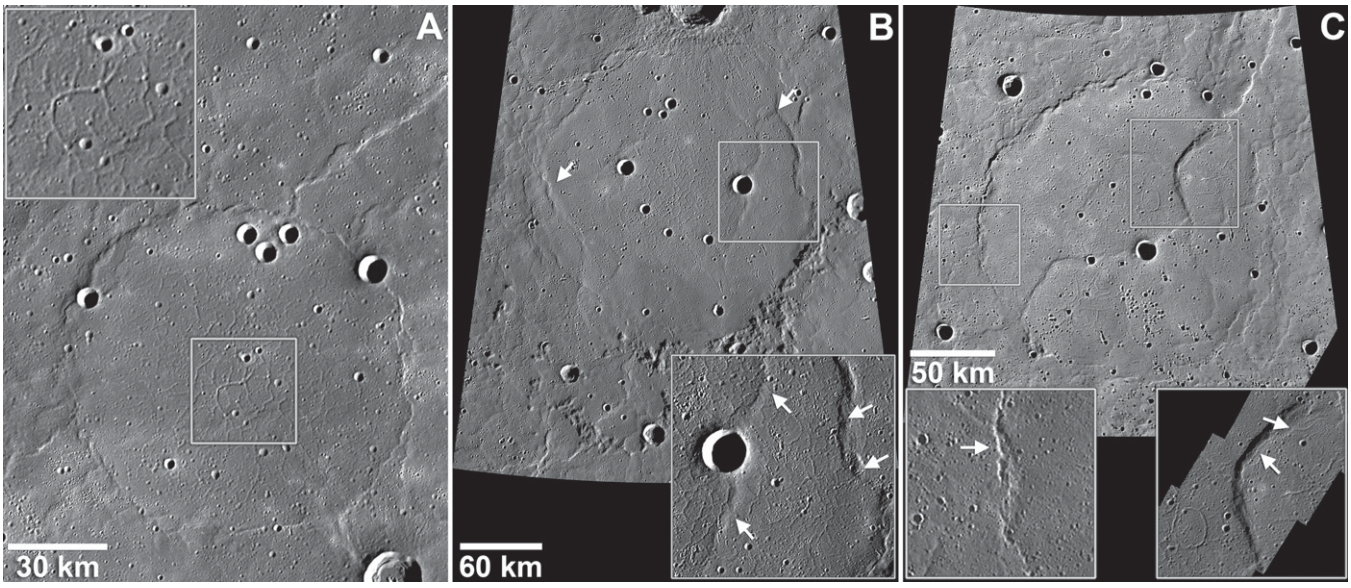

Figure 2. Graben systems interior to wrinkle-ridge rings in the northern volcanic plains; see Figure 1 for locations. A: Graben form a polygonal pattern (inset) and are encircled by a wrinkle-ridge ring ~100 km in diameter and centered at ~60.2°N, 36.5°E. B: Within this ~200-km-diameter partial ridge ring, centered at ~67.2°N, 13.8°E, some graben terminate at or extend onto the flanks of ridges (inset, right arrows), whereas others extend fully across ridges (inset, left arrows). C: Within an outer wrinkle-ridge ring ~170 km in diameter and centered at ~69.5°N, 343.5°E, are three partial ridge rings that enclose graben. Some graben terminate at the ridge flank, and others extend across the crest of a wrinkle-ridge segment of one of the interior rings (right inset, arrows). Segments of the outer ridge ring are superposed on a wrinkle ridge located near the buried basin rim (left inset, arrows).

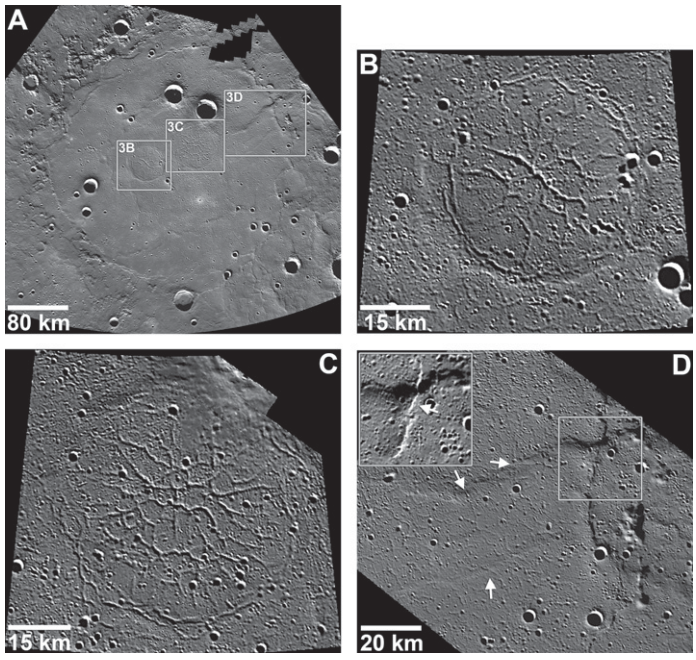

Figure 3. Goethe basin. A: A wrinkle-ridge ring marks the margin of the nearly completely buried basin. Graben are found within two interior ridge rings and throughout the basin fill material. B: The largest graben in Goethe basin are within this ~47-km-diameter ghost crater (location shown in A). Circumferentially oriented graben crosscut the bounding ridge ring. C: Prominent graben extend from the center of this ghost crater (~60 km in diameter; location shown in A), and circumferentially oriented graben crosscut its bounding wrinkle-ridge ring. D: Numerous graben are superposed on and crosscut two approximately northeast–southwest-oriented wrinkle ridges (arrows; location shown in A). Segments of the outer ridge ring appear to be superimposed on a larger, broader wrinkle ridge that extends into the plains beyond the ridge ring (inset, arrow).

example in Figure 2A (up to ~1 km wide, ~10 km in length), but there are wrinkle ridges interior to the ghost crater alongside graben. Some graben terminate at or near the flanks of wrinkle ridges, other graben cut the ridge flanks but do not extend across the ridges (Fig. 2B, inset, right arrows), and still others extend completely across ridges (Fig. 2B, inset, left arrows).

There are also instances where smaller, crater-scale ridge rings are seen within basin-scale ridge rings. These smaller ridge rings, often consisting of discontinuous, arcuate ridge segments, likely indicate the locations of impact craters formed on the basin floor prior to or during the period of flooding of the basin (Head et al., 2011). In one such case (Fig. 2C), the largest graben are generally confined to the areas inside three interior ridge rings with diameters that range from 45 to 60 km. Within the southernmost of these three ghost craters, some graben form polygonal patterns and others are radial or concentric to the bounding ridge ring. The pattern of graben in the central plains, partially encompassed by ridge segments, is polygonal to nearly circular. In one group, graben are oriented radially to the nearest interior ridge ring.

Goethe Basin

The largest expanse of northern plains deformed by graben is within the Goethe basin (centered at ~81°N, 310°E) (Fig. 3A). Goethe is ~300 km in diameter and is almost completely buried by the volcanic material of the northern plains. Only isolated portions and blocks of the basin's rim massifs remain exposed. A nearly continuous wrinkle-ridge ring is located along the basin margin. This ring marks the part of the basin rim that is completely flooded by volcanic plains. Other wrinkle ridges occur within Goethe's ridge ring, including at least three crater-scale ridge rings. The greatest extension within Goethe has occurred within two interior ridge rings near the center of the basin (Fig. 3A). Many of the graben within these interior ghost craters form strongly polygonal patterns, whereas others exhibit distinctly circumferential orientations (Figs. 3B and 3C). The largest graben in the smaller of two interior ridge rings are located near the ring center and are up to ~2 km wide (Fig. 3B). The larger of the interior ridge rings has graben up to ~1.5 km wide, also located near its center

(Fig. 3C). The graben within the ghost craters in Goethe extend to and often across their bounding wrinkle-ridge rings (Figs. 3B and 3C). Graben elsewhere in Goethe appear to be superimposed on wrinkle ridges, and segments of Goethe's outer ridge ring are superimposed on an east–west-trending wrinkle ridge (Fig. 3D).

Temporal Relations

Superposition relations between graben and wrinkle ridges in the Goethe basin and in other ghost craters and basins imply a generally complex evolution of compressional and extensional stresses in the formation of the tectonic systems. Where graben terminate at a ridge flank we regard the ridge as likely having predated graben formation either as a surficial or shallowly buried structure. The relative age of a graben extending across a ridge at a non-orthogonal angle can be determined if the condition of the graben can be established. A graben crosscutting a ridge without modification likely postdates the ridge, whereas modification of the graben indicates that it likely predates the ridge. The available images do not generally exclude either possibility, but we find no clear evidence of modification. Crosscutting relations between distinct wrinkle ridges are interpreted as indicating multiple episodes of ridge formation and development.

MODELING OF STRESS AND DEFORMATION

It is probable that a major source of compressional stress that contributed to wrinkle ridge formation on Mercury was the cooling and contraction of the planet's interior (Strom et al., 1975; Solomon et al., 2008). Another likely source of compressional stress was lithospheric flexure in response to loading by the volcanic plains. Finite element models of the effects of global contraction (see the Data Repository) suggest that circumferential wrinkle ridges should form over buried crater and basin rims because compressional stresses are enhanced by the combined effects of mechanically stronger volcanic units overlying a weaker crust and thinning of the volcanic unit over pre-existing topographic highs (Figs. 4A and 4B). Contributors to a weaker underlying crust include extensive fracturing during the crater-forming impact and any tectonic activity prior to plains emplacement. Under these conditions, stresses within the volcanic unit are approximately inversely proportional to unit thickness and are greatest above buried crater and basin rims. Because global contraction would likely deform any cooled volcanic units, ridge growth at ghost crater rims is expected to have initiated some time after burial and to have continued thereafter. In response to global contraction, wrinkle ridges outside the basin should be more common than within the basin because the exterior volcanic plains are likely thinner and because wrinkle ridges at the basin rim accommodated contractional strain, thereby shielding the basin interior from a portion of the lithospheric contractional stress. Away from buried basin or crater rims, the principal horizontal stresses are similar in magnitude, so no preferred orientation of wrinkle ridges is expected.

Possible sources of extensional stresses that formed the graben include uplift and contraction of the cooling volcanic fill. Uplift can have resulted either from vertical motions that accompanied the long-term isostatic response to crater and basin formation (Dzurisin, 1978; Melosh and Dzurisin, 1978; Blair et al., 2010) or from inward flow of lower crustal material (Watters et al., 2005; Watters and Nimmo, 2010). However, both uplift mechanisms face challenges from timing (the impacts that produced the buried craters and basins hosting interior graben would all have had to closely predate the volcanic infill), and models generally do not predict the pattern of faulting that is observed (see the Data Repository). Moreover, uplift scenarios are problematic for the smaller impact structures, as formation of these features was unlikely to initiate a major isostatic or lower crustal flow response. An additional source of extensional stress may be subsidence-induced flexure of the volcanic unit over buried crater rims.

Contraction of cooling volcanic material has been proposed as a mechanism for the formation of polygonal patterns of extensional fractures on Venus (Johnson and Sandwell, 1992). On Mercury, contraction of the youngest volcanic cooling unit can generate large extensional stresses if the cooling volume experienced resistance to contraction imparted by the strength of underlying layers (Fig. 4C) (see the Data Repository). Without resistance to contraction, a cooling body will develop large contractional strains, but not stresses (though transient stresses will temporarily develop if the body cools non-uniformly). Short of a detachment fault, the underlying units (likely older volcanic flows) should provide substantial resistance to contraction of the youngest cooling unit above. Horizontal extensional stress components are predicted to have been of similar magnitude in regions where the youngest cooling unit is of nearly uniform thickness, so no preferred orientation is predicted for graben (permitting graben that form polygonal patterns). In contrast, in areas where the youngest cooling unit displays a substantial change in thickness, such as over the buried rims of craters or basins, the radial component of thermal stress is more extensional than

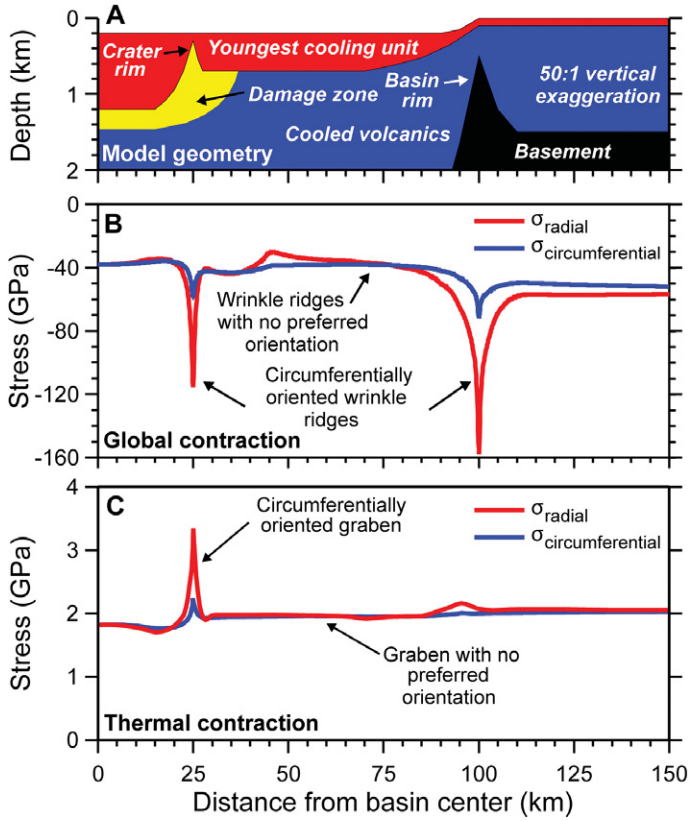

Figure 4. Calculated stresses near the surface of volcanic plains within a buried basin containing an interior ghost crater. A: Model geometry. The youngest cooling unit (red) has buried a 50-km-diameter impact crater, a partially filled 200-km-diameter basin, and surrounding plains. Older, underlying volcanic units (blue) partially filled the basin. The impact is assumed to be underlain by a mechanically weak damage zone (yellow). Brecciated basement rocks (black) are also assumed to be mechanically weaker than the volcanic units. B: Principal horizontal stresses (negative in compression) produced by global cooling and contraction. Global contraction is assumed to shorten horizontally the volcanic unit and the underlying basement by a strain of 4×10^{-4} (corresponding to a 1 km reduction in planetary radius). Thin volcanic deposits above basin and crater rims cause focusing of compressional stresses, promoting the development of a ring of wrinkle ridges. C: Contraction is modeled for a given thickness of the youngest volcanic unit that last cooled below a threshold stress-bearing temperature (~700 °C). The cooling unit can be made up of multiple flows if emplaced within a short (thousands of years) time frame. Older units would have been covered by the younger flows. Stresses due to contraction of the youngest cooling unit can exceed 1 GPa and depend on the resistance to contraction from the underlying units.

the circumferential component, leading to a preferred circumferential orientation for graben (Fig. 4C).

The width of a graben might be expected to be approximately equal to the depth extent of the youngest cooling unit if graben-bounded antithetic normal faults (for symmetric graben and fault dip angles of ~60°) converge at the base of this layer (Melosh and Williams, 1989), but graben are likely asymmetric and their associated faults likely extend to greater depths (e.g., Schultz et al., 2007). The widest graben (expressing the greatest strains), found in Goethe basin (Fig. 3A), have minimum depths of faulting of ~2 km. They occur within buried craters interior to Goethe where pooled lavas presumably were the thickest. Graben in plains within buried basins but outside of interior ghost craters should have lesser widths (perhaps by a factor approaching ~2). The longitudinal extensional strain across the two ghost craters in Goethe is the highest found in the northern plains assemblage (>3%), more than a factor of 2 greater than the average longitudinal strain expressed in deformed plains in Goethe outside the interior ridge rings (Figs. 3A–3C).

CONCLUDING DISCUSSION

On the basis of the finite element models, we suggest that systems of graben and wrinkle ridges within Mercury's northern plains and in the plains exterior to the Caloris basin formed during and following plains emplacement by a combination of local cooling of the plains lavas and global cooling of the planetary interior. After each cooling unit reached its elastic blocking temperature, graben likely formed first because extensional stresses from cooling would have accumulated more rapidly than compressional stresses from global contraction. Wrinkle ridges developed over a much longer time interval, but their underlying fault systems likely continued to be active even for those that were embayed, partially buried, or completely covered by the later lava flows that formed the youngest cooling units. Thus, graben in the youngest cooling unit likely predated the later stages of development of the wrinkle ridges.

Model results show that the calculated strain is proportional to the thickness of the cooling unit, and graben will initiate at a depth proportional to the thickness of the cooling unit (i.e., graben will be deeper and wider in regions where the cooling unit is thickest). The observations of graben in some but not all buried craters and basins may thus indicate that the thickness of the youngest volcanic cooling units is greater in those areas where graben are seen. Moreover, the youngest cooling units covering the volcanic plains where graben are absent may be relatively thin, likely because lavas did not pool to comparable depths.

Thermal contraction modeling is consistent with the emplacement of thick lava flow sequences to form the northern plains (Head et al., 2011) and other major expanses of volcanic plains on Mercury. Data returned by MESSENGER's X-Ray Spectrometer (XRS) indicate that Mercury's average surface composition is intermediate between those of iron-poor basalts and terrestrial komatiites (Nittler et al., 2011). The tectonic systems associated with ghost craters and basins on Mercury may have resulted from the emplacement of low-viscosity lava flows that rapidly accumulated thick cooling units on a planet undergoing a high rate of global contraction. This combination of processes may account for why these tectonic systems are seen on Mercury and not elsewhere. The absence of these tectonic systems, particularly graben due to cooling, on the Moon and Mars, for example, may be because volcanic sequences in lunar maria and Martian ridged plains accumulated over much longer periods than did smooth plains units on Mercury.

ACKNOWLEDGMENTS

We thank W.B. McKinnon, E. Grosfils, and an anonymous reviewer for helpful comments that greatly improved the manuscript. We are grateful to the MESSENGER engineers and technical support personnel. The MESSENGER project is supported by the NASA Discovery Program under contracts NASW-00002 to the Carnegie Institution of Washington and NAS5-97271 to The Johns Hopkins University Applied Physics Laboratory. This work is also supported by NASA grant NNX07AR60G.

REFERENCES CITED

Blair, D.M., Freed, A.M., Melosh, H.J., Solomon, S.C., Prockter, L.M., Watters, T.R., Zuber, M.T., and Phillips, R.J., 2010, Testing mechanisms for the formation of a ring of graben in central Raditladi basin, Mercury: Houston, Texas, Lunar and Planetary Institute, Lunar and Planetary Science 41, abstract 1762, CD-ROM.

Denevi, B.W., Robinson, M.S., Solomon, S.C., Murchie, S.L., Blewett, D.T., Domingue, D.L., McCoy, T.J., Ernst, C.M., Head, J.W., Watters, T.R., and Chabot, N.L., 2009, The evolution of Mercury's crust: A global perspective from MESSENGER: Science, v. 324, p. 613–617.

Dzurisin, D., 1978, The tectonic and volcanic history of Mercury as inferred from studies of scarps, ridges, troughs, and other lineaments: Journal of Geophysical Research, v. 83, p. 4883–4906, doi:10.1029/JB083iB10p04883.

Head, J.W., Murchie, S.L., Prockter, L.M., Robinson, M.S., Solomon, S.C., Strom, R.G., Chapman, C.R., Watters, T.R., McClintock, W.E., Blewett, D.T., and Gillis-Davis, J.J., 2008, Volcanism on Mercury: Evidence from the first MESSENGER flyby: Science, v. 321, p. 69–72, doi:10.1126/science.1159256.

Head, J.W., and 25 others, 2011, Flood volcanism in the northern high latitudes of Mercury revealed by MESSENGER: Science, v. 333, p. 1853–1856, doi:10.1126/science.1211997.

Johnson, C.L., and Sandwell, D.T., 1992, Joints in Venusian lava flows: Journal of Geophysical Research, v. 97, p. 13601–13610, doi:10.1029/92JE01212.

Melosh, H.J., and Dzurisin, D., 1978, Tectonic implications for the gravity structure of Caloris basin, Mercury: Icarus, v. 33, p. 141–144, doi:10.1016/0019-1035(78)90029-5.

Melosh, H.J., and McKinnon, W.B., 1988, The tectonics of Mercury, *in* Vilas, F., Chapman, C.R., and Matthews, M.S., eds., Mercury: Tucson, Arizona, University of Arizona Press, p. 374–400.

Melosh, H.J., and Williams, C.A., 1989, The mechanics of graben formation in crustal rocks: A finite element analysis: Journal of Geophysical Research, v. 94, p. 13961–13973, doi:10.1029/JB094iB10p13961.

Murchie, S.L., Watters, T.R., Robinson, M.S., Head, J.W., Strom, R.G., Chapman, C.R., Solomon, S.C., McClintock, W.E., Prockter, L.M., Domingue, D.L., and Blewett, D.T., 2008, Geology of the Caloris basin, Mercury: A new view from MESSENGER: Science, v. 321, p. 73–76, doi:10.1126/science.1159261.

Nittler, L.R., and 14 others, 2011, The major-element composition of Mercury's surface from X-ray spectrometry: Science, v. 333, p. 1847–1850, doi:10.1126/science.1211567.

Prockter, L.M., and 12 others, 2010, Evidence for young volcanism on Mercury from the third MESSENGER flyby: Science, v. 329, p. 668–671, doi:10.1126/science.1188186.

Robinson, M.S., and 12 others, 2008, Reflectance and color variations on Mercury: Indicators of regolith processes and compositional heterogeneity: Science, v. 321, p. 66–69, doi:10.1126/science.1160080.

Schultz, R.A., Moore, J.M., Grosfils, E.B., Tanaka, K.L., and Mége, D., 2007, The Canyonlands model for planetary grabens: Revised physical basis and implications, *in* Chapman, M. ed., The Geology of Mars: Evidence from Earth-Based Analogs: New York, Cambridge University Press, p. 371–399.

Solomon, S.C., McNutt, R.L., Jr., Watters, T.R., Lawrence, D.J., Feldman, W.C., Head, J.W., Krimigis, S.M., Murchie, S.L., Phillips, R.J., Slavin, J.A., and Zuber, M.T., 2008, Return to Mercury: A global perspective on MESSENGER's first Mercury flyby: Science, v. 321, p. 59–62, doi:10.1126/science.1159706.

Strom, R.G., Trask, N.J., and Guest, J.E., 1975, Tectonism and volcanism on Mercury: Journal of Geophysical Research, v. 80, p. 2478–2507, doi:10.1029/JB080i017p02478.

Watters, T.R., and Nimmo, F., 2010, The tectonics of Mercury, *in* Watters, T.R., and Schultz, R.A., eds., Planetary Tectonics: New York, Cambridge University Press, p. 15–80.

Watters, T.R., Nimmo, F., and Robinson, M.S., 2005, Extensional troughs in the Caloris basin of Mercury: Evidence of lateral crustal flow: Geology, v. 33, p. 669–672, doi:10.1130/G21678.1.

Watters, T.R., Solomon, S.C., Robinson, M.S., Head, J.W., André, S.L., Hauck, S.A., and Murchie, S.L., 2009a, The tectonics of Mercury: The view after MESSENGER's first flyby: Earth and Planetary Science Letters, v. 285, p. 283–296, doi:10.1016/j.epsl.2009.01.025.

Watters, T.R., Murchie, S.L., Robinson, M.S., Solomon, S.C., Denevi, B.W., André, S.L., and Head, J.W., 2009b, Emplacement and tectonic deformation of smooth plains in the Caloris basin, Mercury: Earth and Planetary Science Letters, v. 285, p. 309–319, doi:10.1016/j.epsl.2009.03.040.

Watters, T.R., Head, J.W., Solomon, S.C., Robinson, M.S., Chapman, C.R., Denevi, B.W., Fassett, C.I., Murchie, S.L., and Strom, R.G., 2009c, Evolution of the Rembrandt impact basin on Mercury: Science, v. 324, p. 618–621.

Manuscript received 15 February 2012
Revised manuscript received 7 June 2012
Manuscript accepted 10 June 2012

Printed in USA